Photoelectrochemical Studies of CdS Nanoparticle-Modified Electrodes

Stephen G. Hickey and D. Jason Riley*

School of Chemistry, University of Bristol, Cantock's Close, Bristol BS8 1TS, United Kingdom

Received: January 4, 1999; In Final Form: March 28, 1999

The kinetics of charge transfer at an electrode modified with a submonolayer of CdS nanoparticles is considered using intensity modulated photoelectrochemical spectroscopy (IMPS). First, the method of preparing an electrochemically addressable layer of CdS nanoparticles is detailed. Then a model of charge transfer from nanoparticle-modified electrodes is developed, and equations for the AC photocurrent are derived. Excellent agreement between the experimental and theoretical responses for an electrode coated with nanoparticles of approximately 5-nm radius is obtained. It is demonstrated how rate constants for both hole and electron transfer from semiconductor nanoparticles may be determined.

Introduction

Methods of preparation and studies of the properties of semiconductor nanoparticles is a rapidly expanding area of research.[1−5] The interest in this field results from the novel optical and chemical properties that such nanoparticles display.[1,3,6−8] The relationship between the size of the nanoparticles and their optical properties is well-documented: the band gap increasing with decreasing nanoparticle size as a result of quantum confinement of charge carriers.[9,10] It is envisaged that in the future the ability to control the optical properties of a material by control of particle size will be employed in optoelectronic devices.[11] To achieve this goal, methods of addressing nanoparticles electrically are required.

Recently we,[12] along with a number of other groups,[4,5,13,14] have reported methods of preparing electrodes modified with an electrochemically active layer of CdS nanoparticles. Photocurrent spectroscopy studies show that the surface layer acts as an array of independent nanoparticles; that is, quantum confinement effects are observed. The results reported indicate that photoelectrochemistry offers the possibility of probing the optoelectronic properties of CdS nanoparticles. This paper is concerned with the development of this novel approach. First equations describing the AC photocurrent resulting from modulated illumination of an electrode modified with a submonolayer of CdS nanoparticles are derived. Then the experimental procedure is described. Finally, the experimental results are detailed and analyzed with respect to the theory developed. It is demonstrated that by employing intensity modulated photocurrent spectroscopy (IMPS) information about the kinetics of charge transfer from semiconductor nanoparticles may be obtained.

Theory

The AC photocurrent response of bulk semiconductor electrodes and electrodes coated with semiconductor particle layers to illumination with modulated light has been developed over the past decade.[15−20] When considering such electrodes one must take into account the majority carriers and, in the case of bulk semiconductors, the effects of band bending. For an individual nanoparticle at an electrode surface, the number of dopants is extremely low and the concept of a space charge layer is meaningless; the particle's dimensions are very much smaller than those of a space charge layer. Therefore, for a submonolayer of semiconductor nanoparticles, in which the photoelectrochemical response is that of an array of individual particles, a new theory for the kinetics of photostimulated charge transfer must be developed.

Adsorption of light by a semiconductor nanoparticle results in the formation of an electron−hole pair. Once formed the electron−hole pair may recombine or the charges may be transferred. The latter process will result in a photocurrent. Under a positive bias there is a probability that a conduction band electron may be transferred to the underlying substrate before any recombination occurs. Similarly, a valence band hole may be captured in a surface bond resulting in a photodissolution process. If an efficient hole scavenger is present in the electrolyte, the photodissolution reaction is arrested and the holes are consumed in the oxidation of a solution-phase species. Figure 1 shows a simple model for charge transfer from an illuminated semiconductor nanoparticle under positive bias in the presence of a hole scavenger. The charge-transfer reactions have been assumed to be pseudo-first-order; k_{ET} is the rate constant for electron transfer and k_{HT} is the rate constant for hole transfer. It is supposed that the charge-transfer steps are much faster than any recombination processes.[21,22]

The charge on a particle is given by the expression

$$Q = e(p - n) \tag{1}$$

where p is the number of holes and n is the number of electrons. If the photon flux at a particle (I) is AC modulated such that

$$I = I_{DC} + I_{AC}e^{i\omega t} \tag{2}$$

where I_{DC} is the DC photon flux and I_{AC} is the AC amplitude of the modulated photon flux, then the rate of generation of electron−hole pairs in a nanoparticle (g) is given by the expression

$$g = \alpha(I_{DC} + I_{AC}e^{i\omega t}) \tag{3}$$

where α is the adsorption coefficient of a single particle. Hence

* Corresponding author (e-mail, Jason.Riley@bristol.ac.uk).

10.1021/jp990020r CCC: $18.00
Published on Web 05/14/1999

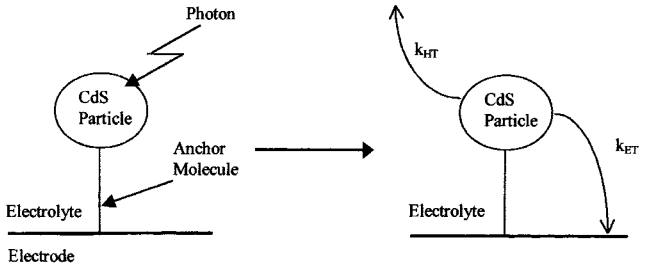

Figure 1. Model for charge transfer from a semiconductor particle at an electrode surface.

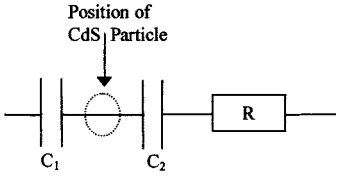

Figure 2. Equivalent circuit for the substrate−nanoparticle−electrolyte interface.

the rate of change in the number of charge carriers per particle is

$$\frac{dn}{dt} = \alpha I_{DC} + \alpha I_{AC} e^{i\omega t} - k_{ET} n \tag{4}$$

for electrons and

$$\frac{dp}{dt} = \alpha I_{DC} + \alpha I_{AC} e^{i\omega t} - k_{HT} p \tag{5}$$

for holes, where n and p are the number of electrons and holes, respectively. It follows that

$$\frac{dq}{dt} = e(k_{ET} n - k_{HT} p) \tag{6}$$

therefore provided that $k_{ET} \neq k_{HT}$ the particle will become charged when illuminated.

An equivalent circuit for the working electrode is shown in Figure 2. Charging of the nanoparticle array results in a change in the potential distribution across the electrode−electrolyte interface. However, the potentiostat maintains a constant potential between the working and reference electrodes; therefore

$$NQ\left(\frac{1}{C_1} + \frac{1}{C_2}\right) = \frac{NQ}{C_T} = jR \tag{7}$$

where C_T is the total capacitance of the nanoparticle, N is the number of nanoparticles in the surface layer, and j is the photocurrent.

Solving eqs 1−7 the AC component of the photocurrent may be determined,

$$j(\omega) = \frac{e g_{AC}(k_{ET} - k_{HT})}{RC_T(k_{HT}^2 + \omega^2)(k_{ET}^2 + \omega^2)} [(k_{ET}k_{HT} - \omega^2) - i\omega(k_{ET} + k_{HT})] \tag{8}$$

At low frequency the plot tends toward the real axis at the limit

$$j(\omega)|_{\omega \to 0} = \frac{e g_{AC}}{RC_T} \frac{(k_{ET} - k_{HT})}{k_{HT}k_{ET}} \tag{9}$$

thus the normalized AC component of the photocurrent is given

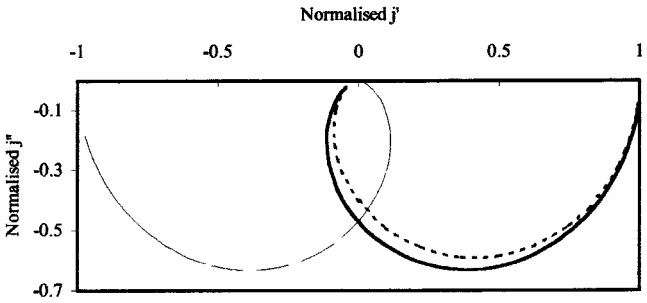

Figure 3. Normalized theoretical IMPS data for different values of k_{ET} and k_{HT} (···, k_{ET} 4000, k_{HT} 1000; —, k_{ET} 2000, k_{HT} 1000; and − − −, k_{ET} 500, k_{HT} 1000).

by the expression

$$j(\omega) = \frac{k_{ET}k_{HT}}{(k_{HT}^2 + \omega^2)(k_{ET}^2 + \omega^2)} [(k_{ET}k_{HT} - \omega^2) - i\omega(k_{ET} + k_{HT})] \tag{10}$$

Normalized IMPS spectra for different values of k_{ET} and k_{HT} are displayed in Figure 3. The plots indicate that if $k_{ET} > k_{HT}$ the low-frequency intercept is at positive real values, while a negative intercept is observed if $k_{ET} < k_{HT}$. As the frequency increases the imaginary component of the AC photocurrent passes through a maximum. At high frequency the response tends to zero as the AC component of the photocurrent becomes completely attenuated. As the modulated photocurrent approaches zero it crosses the imaginary axis at

$$\omega = \sqrt{k_{ET}k_{HT}} \tag{11}$$

It is evident that careful fitting of the data obtained during an IMPS study of a semiconductor nanoparticle-modified electrode surface permits the determination of unique values for the rate constants of the individual tunneling events.

Experimental Section

A detailed description of the method employed to prepare the CdS nanoparticle-modified electrodes has recently been published.[12] The two steps involved in the process are briefly outlined below. First the surface of a tin oxide electrode is functionalized using (3-mercaptopropyl)trimethoxysilane (MPTMS) to yield a surface with pendent thiol groups. Second, hexanethiol-stabilized CdS nanoparticles are formed by bubbling hydrogen sulfide into a 1×10^{-3} mol dm^{-3} $Cd(ClO_4)_2$ solution of THF. If the second step is performed in the presence of a thiol-functionalized surface, then an electrode modified with a submonolayer of CdS nanoparticles results. It has been demonstrated that the size of the nanoparticles can be controlled by varying the stabilizer-to-reactant ratio. This paper is concerned with CdS nanoparticle-modified electrodes on which the particles have a radius of 5 nm.

All electrochemical experiments were performed in a buffered pH 12 1 mol dm^{-3} aqueous Na_2SO_3 solution. Such a solution is known to suppress the photodissolution of CdS. Potential control of the modified electrode−electrolyte interface was achieved using a potentiostat in three-electrode mode: a platinum gauze counter electrode and a silver/silver chloride reference electrode. All potentials are reported relative to the silver/silver chloride reference electrode.

Initial electrochemical characterization of the CdS nanoparticle-modified electrodes was performed in the dark. Cyclic voltammograms of both the thiol-functionalized and the modi-

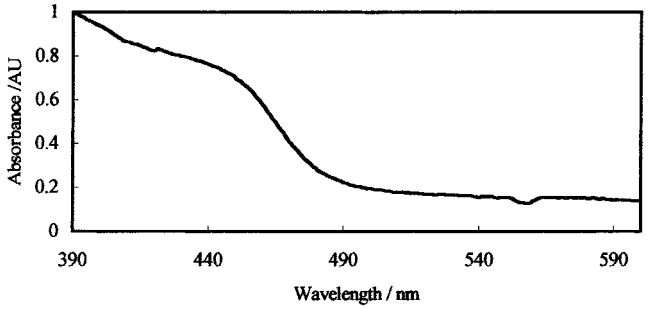

Figure 4. UV−vis spectrum of the thiol-stabilized CdS particles in THF (r = 5 nm) normalized to the absorbance value at 390 nm.

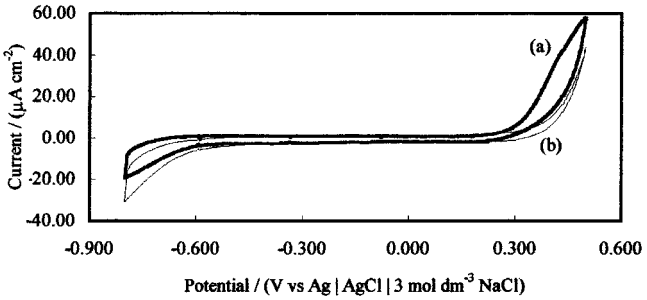

Figure 5. Dark CV of both the CdS-modified (a) and the MPTMS-functionalized (b) electrodes (electrolyte: 1 mol dm^{-3} Na_2SO_3 buffered to pH 12, scan rate 50 mV s^{-1}).

fied electrodes were recorded. The impedance of the cell was also measured; a Solartron 1250/Solartron 1286/Z-Plot impedance apparatus was employed. An AC amplitude of 5 mV was applied, and the frequency was swept between 65 kHz and 1 Hz.

The transfer kinetics of photogenerated charge carriers was investigated in a series of photoelectrochemical studies. Photocurrent spectra were recorded using a xenon light source and monochromator; the light was chopped at a frequency of approximately 17 Hz and the modulated current signal recorded using a lock-in amplifier. IMPS studies were performed using a focused 470-nm LED as the light source; the area of electrode under illumination was 0.5 cm^2. The modulation amplitude of the incident light and the frequency were controlled via a Solartron 1250 frequency response analyzer. Typically a modulation amplitude corresponding to 10% peak-to-peak of the DC light intensity was employed, and the frequency was swept between 4 kHz and 4 Hz.

Results and Discussion

The UV−vis spectrum of the solution-phase CdS nanoparticles formed during electrode preparation is shown in Figure 4. The adsorption spectrum obtained indicates that the band gap of the particles is 2.42 eV; that is, the nanosized particles have bulk optical properties. It should be noted that the absorbance does not go to zero at long wavelengths; this is a result of light scattering by the colloidal particles.

Cyclic voltammograms, recorded in the dark, for both a MPTMS-coated electrode and a CdS nanoparticle-modified electrode are shown in Figure 5. It is apparent that the dark current from the electrodes is dominated by the underlying substrate. Hence, electrochemical data on the CdS nanoparticles can only be obtained using photoelectrochemical techniques. A photocurrent spectrum for a CdS nanoparticle-modified electrode is displayed in Figure 6a. The similarity between the UV−vis spectrum and the photocurrent spectrum indicates that the photoactivity of the electrode is due to the CdS nanoparticles.

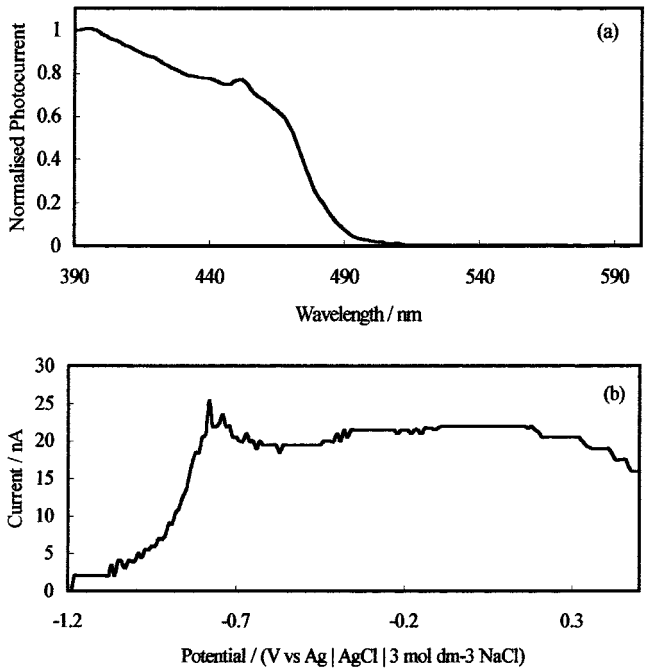

Figure 6. (a) Photoelectrochemical spectrum of the CdS-modified electrode (r = 5 nm, electrolyte: 1 mol dm^{-3} Na_2SO_3 buffered to pH 12). (b) Photocurrent as a function of applied potential for the CdS-modified electrode (r = 5 nm, electrolyte: 1 mol dm^{-3} Na_2SO_3 buffered to pH 12).

The band gap may be more easily determined from the photocurrent measurement as there is no light scattering phenomenon at long wavelengths. Figure 6b shows the photocurrent as a function of potential for an electrode illuminated with 470-nm radiation; the photocurrent onset potential is −1.1 V. This potential is slightly above the reported flatband potential of single-crystal CdS in the same solution.

The IMPS analysis of the CdS nanoparticle-modified electrodes was performed at an applied potential of 0.2 V, in the plateau region of the photocurrent versus applied potential curve. The experimental normalized AC component of the photocurrent as a function of frequency is shown in Figure 7. Detailed analysis of the complex photocurrent response is discussed below. At this stage two features of the complex photocurrent plot should be noted. First, the imaginary part of the photocurrent is negative; this is in contrast with the photocurrent observed at a CdS single-crystal electrode where the imaginary part of the photocurrent is positive across the entire frequency range due to majority carrier transport effects. Second, the photocurrent crosses the real axis, indicating a time delay in the transport of charge carriers from the nanoparticle to the underlying substrate.

The similarity between the experimental plot in Figure 7 and the theoretical data displayed in Figure 3 is apparent. Hence it may be concluded that the AC current flowing when the CdS nanocrystalline surface is illuminated with a modulated light source is due to charge-transfer processes and not photoconductivity effects. The latter cannot account for the observed experimental response. The IMPS data can be satisfactorily fitted using eq 10. The rate constants obtained for hole and electron transfer are 2.8×10^3 and 5.1×10^3 s^{-1}, respectively. The agreement between theory and experiment is shown in Figure 7. A deviation between the two plots is apparent at low frequency; this may be due to slow recombination processes which have not been taken into account.

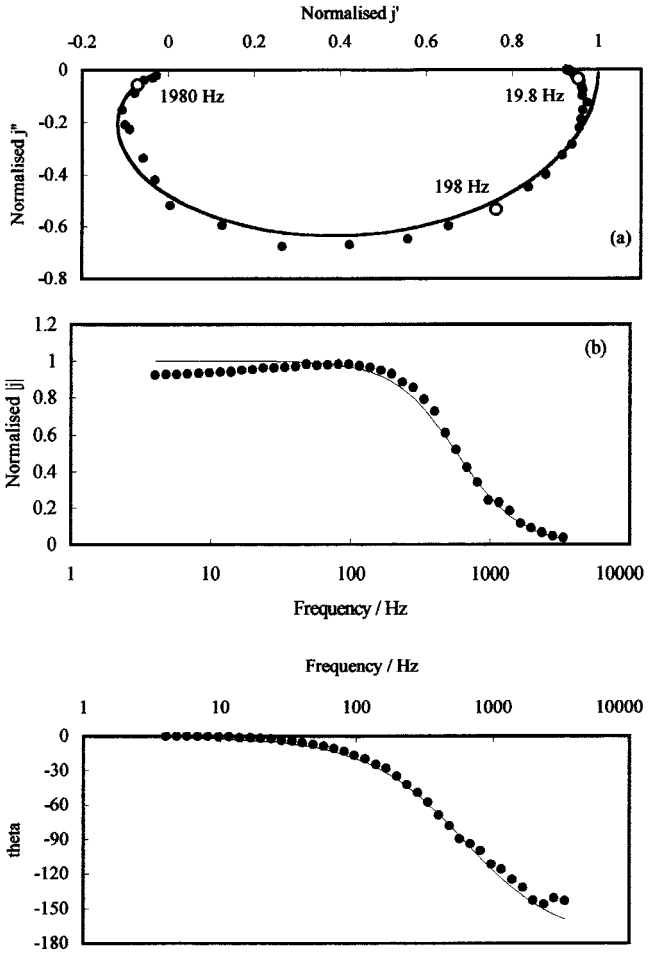

Figure 7. Complex plane and Bode plots of the experimental (●) and theoretical (line) data for CdS particles of radius 5 nm. All values are normalized at the point where I_{theory} crosses the *x* axis (applied potential = 0.2 V, frequency range from 4 kHz to 4 Hz).

Conclusions

A novel method of probing the optical properties of electrically addressable semiconductor nanoparticles has been developed. The method is based on IMPS studies of electrodes modified with submonolayers of CdS nanoparticles. Theory has been adapted to describe the AC component of the photogenerated current at a semiconductor-modified electrode under modulated illumination. Experimental studies of electrodes modified with submonolayers of CdS show that the technique allows the rate constants for electron and hole transfer to be determined. The approach should be particularly useful in the investigation of the effects of quantum confinement and potential on charge-transfer rate constants.

Acknowledgment. S.G.H. gratefully acknowledges the EPSRC for a studentship. This work was also supported by the Nuffield Foundation.

References and Notes

(1) Henglein, H. *Chem. Rev.* **1989**, *89*, 1861.
(2) Fisher, C. H.; Henglein, H. *J. Phys. Chem.* **1989**, *93*, 5578.
(3) Weller, H. *Angew. Chem., Int. Ed. Engl.* **1993**, *32*, 41.
(4) Zhao, X. K.; McCormick, L.; Fendler, J. H. *Chem. Mater.* **1991**, *3*, 922.
(5) Nakanishi, T.; Ohtani, B.; Uosaki, K. *J. Phys. Chem. B* **1998**, *102*, 1571.
(6) Brus, L. E. *Appl. Phys. A* **1991**, *53*, 465.
(7) Wang, Y.; Herron, N. *J. Phys. Chem.* **1991**, *95*, 525.
(8) Weller, H. *Angew. Chem.* **1993**, *105*, 43.
(9) Baral, S.; Fojtik, A.; Weller, H.; Henglein, A. *J. Am. Chem. Soc.* **1986**, *108*, 375.
(10) Vossmeyer, T.; Katsikas, L.; Giersig, M.; Popovic, I. G.; Diesner, K.; Chemseddine, A.; Eychmuller, A.; Weller, H. *J. Phys. Chem.* **1994**, *98*, 7665.
(11) Feldheim, D. L.; Keating, C. D. *Chem. Soc. Rev.* **1998**, *27*, 1.
(12) Drouard, S.; Hickey, S. G.; Riley, D. J. *Chem. Commun.* **1999**, 67.
(13) Nakanishi, T.; Ohtani, B.; Shimazu, K.; Uosaki, K. *Chem. Phys. Lett.* **1997**, *278*, 233.
(14) Ogawa, S.; Fan, F. F.; Bard, A. J. *J. Phys. Chem.* **1995**, *99*, 11182.
(15) Ponomarev, E. A.; Peter, L. M. *J. Electroanal. Chem.* **1995**, *396*, 219.
(16) Ponomarev, E. A.; Peter, L. M. *J. Electroanal. Chem.* **1995**, *397*, 45.
(17) Gomes, W. P.; Vanmaekelbergh, D. *Electrochim. Acta* **1996**, *41*, 967.
(18) de Jongh, P. E.; Vanmaekelbergh, D. *Phys. Rev. Lett.* **1996**, *77*, 3427.
(19) de Jongh, P. E.; Vanmaekelbergh, D. *J. Phys. Chem. B* **1997**, *101*, 2716.
(20) Kelly, J. J.; Vanmaekelbergh, D. *Electrochim. Acta* **1998**, *43*, 2773.
(21) Inoue, T.; Watanabe, T.; Fujishima, A.; Honda, K.; Kohayakawa, J. *J. Electrochem. Soc.* **1977**, *124*, 719.
(22) Albery, W. J.; Bartlett, P. N.; Porter, J. D. *J. Electrochem. Soc.* **1984**, *131*, 2897.